

Anisotropy of Vortex-Liquid and Vortex-Solid Phases in Single Crystals of $\text{Bi}_2\text{Sr}_2\text{CaCu}_2\text{O}_{8+\delta}$: Violation of the Scaling Law

J. Mirković*, S. E. Savel'ev, E. Sugahara, and K. Kadowaki
Institute of Materials Science, University of Tsukuba, Tsukuba 305-8573, Japan

The vortex-liquid and vortex-solid phases in single crystals of $\text{Bi}_2\text{Sr}_2\text{CaCu}_2\text{O}_{8+\delta}$ placed in tilted magnetic fields are studied by in-plane resistivity measurements using the Corbino geometry to avoid spurious surface barrier effects. It was found that the anisotropy of the vortex-solid phase increases with temperature and exhibits a maximum at $T \approx 0.97 T_c$. In contrast, the anisotropy of the vortex-liquid rises monotonically across the whole measured temperature range. The observed behavior is discussed in the context of dimensional crossover and thermal fluctuations of vortices in the strongly layered system.

The anisotropic static and dynamical properties of superconductors have commonly been described by the three-dimensional Ginzburg-Landau (hereafter 3DGL) theory with a single parameter of anisotropy γ defined as a ratio $(m_c/m_{ab})^{1/2}$ of the effective masses m_c and m_{ab} along the c -axis and in the ab -plane, respectively [1]. The anisotropy is related to the basic parameters of a superconductor as $\gamma = \xi_{ab}/\xi_c = \lambda_c/\lambda_{ab} = H_{c2\parallel}/H_{c2\perp}$, where ξ_{ab} and ξ_c are the in-plane and the out-of-plane coherence lengths, λ_c and λ_{ab} are the magnetic field penetration depths along the c -axis and in the ab -plane, while $H_{c2\perp}$ and $H_{c2\parallel}$ are the out-of-plane and the in-plane upper critical magnetic fields.

Based on 3DGL, Blatter *et al.* [2] obtained the general scaling law, which can be applied for the description of different physical properties of anisotropic superconductors in oblique magnetic fields. For instance, the resistivity in a magnetic field H , tilted away from the c -axis for the angle θ , depends only on the reduced field as

$$\rho(H, \theta) = \rho(H \sqrt{\cos^2 \theta + \sin^2 \theta / \gamma^2}). \quad (1)$$

The scaling law for the vortex lattice melting magnetic field was derived in a similar manner as

$$H^{melt}(\theta) = H^{melt}(\theta = 0) / \sqrt{\cos^2 \theta + \sin^2 \theta / \gamma^2}. \quad (2)$$

In previous studies it was found that the scaling law describes well experimental data such as resistivity [3,4], magnetization [5], and thermodynamic measurements [6] in $\text{YBa}_2\text{Cu}_3\text{O}_{7-\delta}$ with anisotropy parameter $\gamma \approx 5 - 7$ [1]. Concerning the higher anisotropic layered systems, it was recognized earlier that the dissipation in $\text{Bi}_2\text{Sr}_2\text{CaCu}_2\text{O}_{8+\delta}$ depends practically only on the c -axis magnetic field component [7,8] except very close to the ab -plane [9] which is in agreement with the 3DGL scaling law with high anisotropy parameter. However, it was reported [10] that the resistivity data near the ab -plane agree better with Thinkam's thin film (hereafter 2DT) model [11], than with the 3DGL theory. Later, it was also found that the measured anisotropy parameter for $\text{Bi}_2\text{Sr}_2\text{CaCu}_2\text{O}_{8+\delta}$ thin films increases with temperature, according to the 2DT model, followed by an indication of the two to three-dimensional (2D-3D) crossover near the

transition temperature T_c [12,13]. On the other hand, recent experimental studies of the first-order vortex-lattice melting transition (hereafter VLMT) have shown a linear decay of the out-of-plane melting field with an increasing in-plane magnetic field, even near the c -axis [14,15], in a strong contrast to the above mentioned approaches. In a strict sense, it is reasonable to expect that the scaling law based on the 3DGL model may not be applicable to the extremely anisotropic layered system such as $\text{Bi}_2\text{Sr}_2\text{CaCu}_2\text{O}_{8+\delta}$. In this material, the coherence length along the c -axis at low temperatures is smaller than the lattice parameters of the crystal, which means that the layeriness of the material has to be considered [1]. Thus, the 3DGL scaling approach [2], based on a continuous medium, is not valid due to the discreteness of the system, and therefore, it is not at all trivial that the expressions (1) and (2) are still valid.

Hence, there is still a question of how the anisotropy manifests itself in the different vortex phases in $\text{Bi}_2\text{Sr}_2\text{CaCu}_2\text{O}_{8+\delta}$ single crystals. In this Letter, we report the comparative study of the anisotropy of the vortex-solid and vortex-liquid phases in single crystals of $\text{Bi}_2\text{Sr}_2\text{CaCu}_2\text{O}_{8+\delta}$. The anisotropy of the first-order vortex lattice melting transition increases with temperature in the range of $T < 0.97 T_c$, whereas at higher temperatures, the VLMT anisotropy decreases. In contrast to the anisotropy of the VLMT, the anisotropy of the in-plane resistivity in the vortex liquid phase increases monotonically with temperature in the whole measured range.

The in-plane resistivity measurements were performed for three as-grown single crystals of $\text{Bi}_2\text{Sr}_2\text{CaCu}_2\text{O}_{8+\delta}$ with transition temperatures $T_c^{(I)} = 90.3$ K, $T_c^{(II)} = 86.0$ K, and $T_c^{(III)} = 90.0$ K, for the samples #s1, #s2 and #s3, respectively. In order to probe the true bulk properties, *i.e.*, to avoid the surface barrier effects which occur in conventional strip geometry [16], we have used the Corbino electrical contact configuration (see inset in Fig. 1a). The diameters of the Corbino discs were $D^{(I)} = 1.9$ mm, $D^{(II)} = 1.95$ mm, and $D^{(III)} = 2.7$ mm while the thickness was $t \approx 20$ μm for all samples. The resistance has been measured by using the ac lock-in technique at a low frequency of 37 Hz. The magnetic field, generated up to 70 kOe by a superconducting split

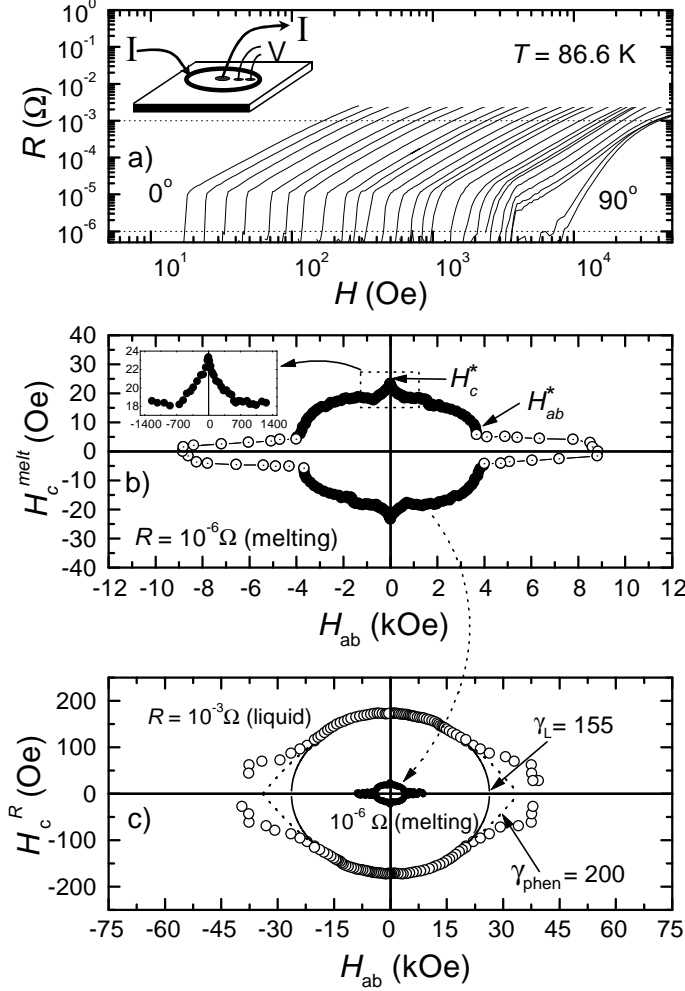


FIG. 1. (a) The magnetic field dependence of the resistance at various field orientations from $\mathbf{H} \parallel \mathbf{c}$ (0°) to $\mathbf{H} \parallel \mathbf{ab}$ (90°) at $T=86.6$ K (sample #s1). Inset in (a): electrical contacts in the Corbino geometry. (b) The $H_c - H_{ab}$ phase diagram of the vortex lattice melting transition at $T = 86.6$ K: the filled symbols mark the first-order phase transition, while the open ones correspond to the continuous resistivity transition. Inset in (b): the part of the VLMT phase diagram near the c -axis, plotted at a magnified scale. (c) The equi-resistance contour at 86.6 K (open symbols) in the vortex-liquid phase. The melting transition from (b) is replotted at the centre. The solid line is the ellipse with anisotropy value of $\gamma_L = 155$, while the dotted line corresponds to the phenomenological formula with $\gamma_{phen} = 200$.

magnet, was rotated by a fine goniometer with angular resolution of 0.01° .

A typical set of the resistance curves is presented in Fig. 1a for $T = 86.6$ K. The sharp resistance drop, attributed to the VLMT [17], is clearly detected across the wide angular range ($\theta < 89.86^\circ$) [15]. Using the resistance criteria of $R = 10^{-6}\Omega$, which is set somewhat below

the resistivity kink, and $R = 10^{-3}\Omega$, which is well above the VLMT anomaly, we construct the phase diagram of the VLMT and the equi-resistance contour for the vortex-liquid in the $H_c - H_{ab}$ phase plane (Fig. 1(b,c)). The VLMT phase line $H_c^{\text{melt}}(H_{ab})$ (Fig. 1b) exhibits the peculiar step-wise shape [15]. Namely, starting from the c -axis, the out-of-plane component of the VLMT, H_c^{melt} , decays linearly with increasing H_{ab} [14], which is associated with the crossing vortex lattice [18]. As the magnetic field further approaches the ab -plane, the linear dependence $H_c^{\text{melt}}(H_{ab})$ sharply transforms to the plateau (inset in Fig.1 b), which is attributed to the trapping of pancake vortices by Josephson vortices [19]. Very close to the ab -plane ($\theta \approx 89.96^\circ$), the first-order phase transition (filled symbols in Fig. 1b) changes to the continuous resistance transition (open symbols), which exhibits the cusp in the $H_c - H_{ab}$ phase plane [15]. In strong contrast to the linear decay of $H_c^{\text{melt}}(H_{ab})$ around the c -axis, the equi-resistance line $H_c^R(H_{ab})$ (Fig. 1c) in the vortex-liquid phase demonstrates smooth quadratic behavior. Near the ab -plane, the equi-resistance contour still has a tail, as if it traces the VLMT cusp. The cusp-like shape of both the VLMT line and the equi-resistance contour, pronounced near the ab -plane, is possibly associated with the intrinsic pinning [20] which, surprisingly, seems to be active even in the vortex liquid phase, quite far from the VLMT.

The next question is how to estimate the anisotropy of the vortex liquid phase and the VLMT. The smooth quadratic dependence $H_c^R(H_{ab})$, can be derived from the general symmetry law $\rho(H_c, H_{ab}) = \rho(H_c, -H_{ab})$, assuming that the resistivity is an analytical function of H_{ab} in the vortex-liquid. The simple analysis [21] gives the angular dependence $H_c^R(H_{ab}) = H_c^R(0) - H_{ab}^2 / (H_c^R(0)\gamma_{phen}^2)$ for the limited angular range $0^\circ < \theta < 90^\circ - 57.3^\circ / \gamma_{phen}$ with phenomenological anisotropy parameter $\gamma_{phen}(T, H_c)$. This equation successfully fits our data at 86.6 K in the vortex liquid phase except very close to the ab -plane with $\gamma_{phen} = 200$ (dotted line in Fig. 1c). It is worth noting that the phenomenological angular dependence $H_c^R(H_{ab})$ coincides with the angular dependence of the upper critical field $H_{c2}(\theta)$ for thin superconducting films obtained by Tinkham [11] as $H_{c2}(\theta) \cos \theta / H_{c2\perp} + H_{c2}^2(\theta) \sin^2 \theta / \gamma_{2DT}^2 H_{c2\perp}^2 = 1$ with the field independent anisotropy parameter $\gamma_{2DT} \propto 1/\sqrt{1 - T/T_c}$. On the other hand, to describe the equi-resistance contours in the vortex liquid phase, it is convenient to apply the more common 3DGL model. Following the 3DGL theory, the $H_c^R(H_{ab})$ line should be an ellipse $(H_c^R(H_{ab}))^2 + H_{ab}^2 / \gamma_{3DGL}^2 = (H_c^R(0))^2$ with anisotropy γ_{3DGL} being independent of magnetic field and temperature. Fitting the curve in Fig. 1c to an ellipse with an anisotropy parameter of 155, we also find a reasonable agreement only in a limited angular range $\theta < 89.75^\circ$. Moreover, the empirical anisotropy γ_L of the vortex liquid, obtained by the elliptical fitting of the equi-

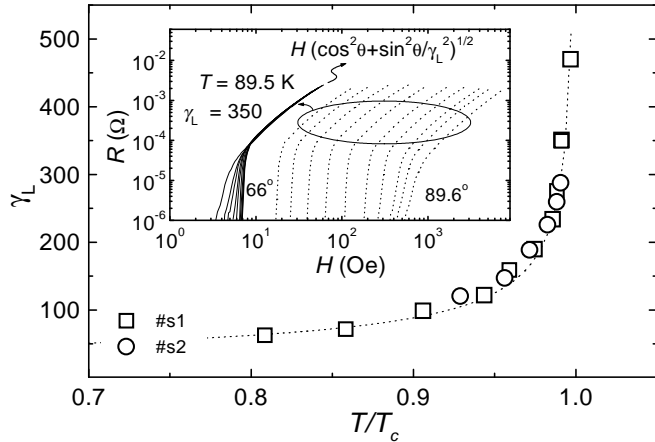


FIG. 2. The temperature dependence of γ_L , extracted by fitting the equi-resistance lines to an ellipse, for samples #s1 and #s2. The dashed line corresponds to the dependence $\gamma_L = 28/(1 - T/T_c)^{1/2}$. Inset: The dotted curves show the $R(H)$ data obtained at $T=89.5$ K at various magnetic field orientations with respect to the c -axis (from left, $\theta = 66^\circ, 74^\circ, 80^\circ, 84^\circ, 86.5^\circ, 88.05^\circ, 88.75^\circ, 89.2^\circ, 89.39^\circ, 89.6^\circ$). The solid curves represent scaled resistance curves according to equation (1) with $\gamma = \gamma_L = 350$.

resistance contours, increases strongly with temperature in the whole measured temperature interval (Fig. 2), which indicates that the 3DGL scaling law is violated. Thus, the anisotropy parameter γ_L extracted from the ellipse can no longer be attributed to the ratio of the effective masses as assumed in the 3DGL theory and may reflect the two-dimensional character of the vortex system in analogy to the 2DT approach [11]. Interestingly, the resistivity curves above the VLMT kink, measured at different field orientations ($\theta < 89.6^\circ$, $T = 89.5$ K, $R < 2 \cdot 10^{-3}\Omega$), collapse into a unique one if the curves $R(H, \theta)$ are scaled in a common way by using eq. (1) (see inset in Fig. 2) with $\gamma = \gamma_L$. Hence, the anisotropy depends weakly on the resistance level in the vortex liquid but changes sharply around the vortex-lattice melting transition (see Inset in Fig. 2), implying different dimensionality of the probed vortex phases.

Recognizing the fact that the VLMT does not follow the 3D scaling law (2), the effective anisotropy of the VLMT can be estimated by the ratio $\gamma_{melt} = H_{ab}^*/H_c^*$ (for definition of H_c^* and H_{ab}^* , see Fig. 1b). It is necessary to emphasize that the VLMT phase lines, obtained at different temperatures, fall roughly on a unique line if plotted in the phase plane $H_c/H_c^* - H_{ab}/H_{ab}^*$, as shown in Fig. 3a. Therefore, the whole VLMT line in the $H_c - H_{ab}$ plane changes proportionally with temperature, which justifies the chosen definition of the anisotropy of the VLMT. The temperature dependences of the

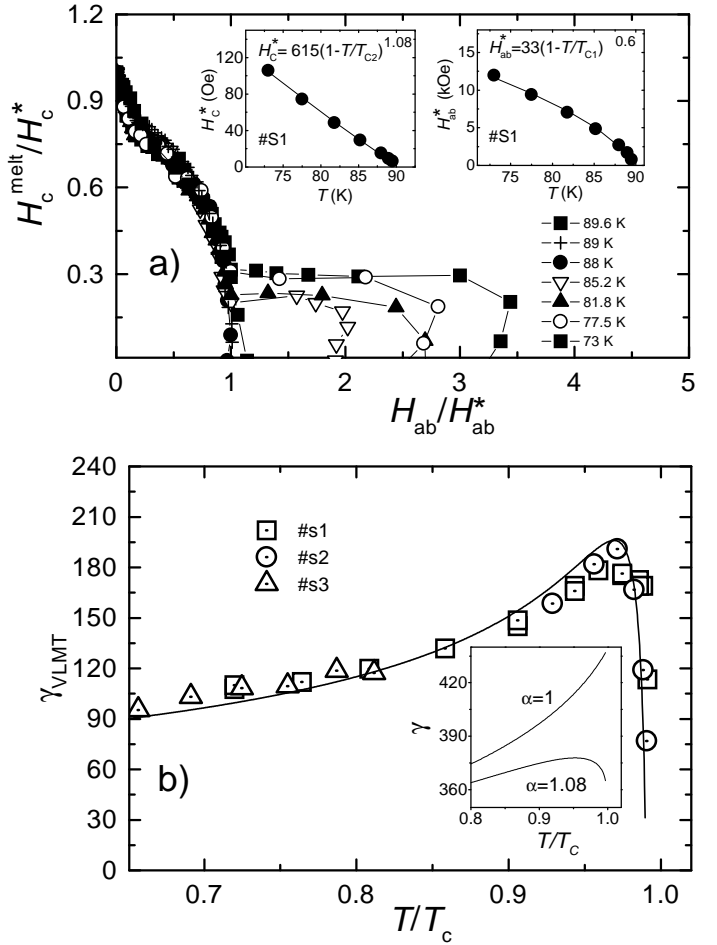


FIG. 3. (a) The phase diagrams of the vortex melting transition plotted in the phase plane $H_c/H_c^* - H_{ab}/H_{ab}^*$ at different temperatures for #s1. The left and right insets display the temperature dependence of H_{ab}^* and H_c^* , respectively (for definition of the fields H_{ab}^* and H_c^* , see Fig. 1b). (b) The temperature dependence of the VLMT anisotropy defined as $\gamma_{melt} = H_{ab}^*/H_c^*$, obtained for three samples. The solid line is the empirical equation for $\gamma_{melt}(T)$ discussed in the text. Inset: the calculated temperature dependence of the anisotropy in the frame of the model [23].

characteristic fields H_c^* and H_{ab}^* exhibit different curvatures (see insets in Fig. 3a), which result in a maximum of the temperature dependence of the VLMT anisotropy $\gamma_{melt}(T)$ at $T \approx 0.97 T_c$ as it is seen in Fig 3b. The obtained temperature dependence of γ_{melt} may be approximated by the empirical equation $\gamma_{melt}(T) = \gamma_0(1 - T/T_{c1})^\beta / (1 - T/T_{c2})^\alpha$ (the solid line in Fig. 3b) with parameters $T_{c1} = 89.4$ K, $T_{c2} = 90.7$ K, $\alpha = 1.08$ and $\beta = 0.6$ obtained by fitting the fields $H_c^*(T) = H_c^*(0)(1 - T/T_{c2})^\alpha$ and $H_{ab}^*(T) = H_{ab}^*(0)(1 - T/T_{c1})^\beta$ for the sample #s1. The two characteristic tempera-

tures (T_{c1} , T_{c2}) in the above empirical formula, may appear due to the fact that the thermodynamical vortex fluctuations have different influence on the interlayer and the intralayer-superconductivity in the tilted magnetic fields. The similar maximum of $\gamma(T)$, accompanied by the disappearance of the cusp in the dependence $H_{onset}(\theta)$ ($R(H_{onset}) = 0$) near the ab -plane, was observed earlier in thin films of $\text{Bi}_2\text{Sr}_2\text{CaCu}_2\text{O}_{8+\delta}$ [12], although there was neither indication of the VLMT nor clear evidence which vortex phase was probed. The phenomenon [12] was interpreted [13] as a crossover from 2D to 3D behavior, which occurs when the coherence length ξ_c exceeds the distance between CuO_2 layers. In agreement with this scenario, the cusp in the $H_c - H_{ab}$ phase diagram, associated with the continuous resistivity transition, also disappears around the temperature (see Fig. 3a) at which $\gamma_{melt}(T)$ is at a maximum [22]. However, based on the 2D-3D crossover, it is impossible to explain why the anisotropy of the vortex liquid phase still increases at temperatures $T > 0.97 T_c$ where $\gamma_{melt}(T)$ decreases. Moreover, the 2D-3D scenario proposed in [13] describes only the temperature and angular dependence of the upper critical field $H_{c2}(\theta, T)$, which, strictly speaking, can not be applied to the VLMT and the equi-resistance contours.

Another possible origin of the temperature dependence of the anisotropy could be related to the thermal fluctuations of vortices, which suppress the Josephson coupling in-between the CuO_2 layers more efficiently than the superconductivity within the layers. As a result, $\lambda_c(T)$ increases faster than $\lambda_{ab}(T)$ and, thus, the anisotropy $\gamma = \lambda_c/\lambda_{ab}$ rises with increasing temperature. According to the model proposed for the magnetic field parallel to the c -axis [23], the temperature dependence of the anisotropy is determined by the equation $\gamma^2/\gamma_0^2 = \exp(\delta(H_c, T)\gamma^2/\gamma_0^2)$ [24], where $\delta = \pi T H_c s \lambda_{ab}^2(T) \gamma_0^2 / 2 \Phi_0^3$ with $\gamma_0 = \gamma(T = 0)$. In order to take into account the temperature dependences of the VLMT and equi-resistance magnetic fields, the empirical equation $H_c = H_0(1 - T/T_c)^\alpha$ is used. Since γ is a monotonical function of $\delta \propto T(1 - T/T_c)^{\alpha-1}$, the temperature dependence of γ has a maximum approaching T_c , if $\alpha > 1$, otherwise γ monotonically increases with T . The inset in Fig. 3b displays the temperature dependence of γ obtained by using the above equations with $\gamma_0 = 300$ and $\alpha = 1.08$, corresponding to the measured VLMT (inset in Fig. 3b), and $\alpha = 1$, as assumed for the vortex-liquid phase. Nevertheless, the calculated value of the magnetic field $H_0 = 29$ kOe disagrees with the experimental value of the c -axis field component, but is close to the total applied magnetic field. The discrepancy could be related to the presence of the Josephson vortices, which have not been considered in the model [23]. The pancake vortex sublattice interacts with the Josephson vortex sublattice in the crossing lattice structure (set in the tilted

magnetic fields) providing the additional mechanism of the renormalization of the anisotropy in the vortex-solid phase [18,19].

In summary, in contrast to the prevailing belief, we have found clear experimental evidence that neither the 3DGL scaling law nor the 2D Tinkham's model consistently describe the resistivity in the vortex-liquid phase as well as the behavior of the vortex lattice melting transition, which can qualitatively be accounted for by the thermal fluctuations of vortices.

We thank M. Tachiki, L. N. Bulaevskii, A. E. Koshelev, and V. M. Vinokur for stimulating discussions.

* Faculty of Sciences, University of Montenegro, P.O. Box 211, 81000 Podgorica, Montenegro, Yugoslavia

- [1] G. Blatter *et al.*, Rev. Mod. Phys. **66**, 1125 (1994).
- [2] G. Blatter *et al.*, Phys. Rev. Lett. **68**, 875 (1992).
- [3] Y. Iye *et al.*, Physica **C166**, 62 (1990).
- [4] W. K. Kwok *et al.*, Phys. Rev. Lett. **69**, 3370 (1992).
- [5] U. Welp *et al.*, Phys. Rev. B **40**, 5263 (1989).
- [6] A. Schilling *et al.*, Phys. Rev. **B58**, 11157 (1998).
- [7] P. H. Kes *et al.*, Phys. Rev. Lett. **64**, 1063 (1990).
- [8] Y. Iye *et al.*, Physica **C159**, 433 (1989).
- [9] H. Raffy *et al.*, Phys. Rev. Lett. **66**, 2515 (1991).
- [10] M. J. Naughton *et al.*, Phys. Rev. B **38**, 9280 (1988).
- [11] M. Tinkham, Phys. Rev. **129**, 2413 (1963).
- [12] E. Silva *et al.*, Phys. Rev. B **55**, 11115 (1997).
- [13] S. Sarti *et al.*, Phys. Rev B **49**, 556 (1994).
- [14] S. Ooi *et al.*, Phys. Rev. Lett. **82**, 4308 (1999).
- [15] J. Mirković *et al.*, Phys. Rev. Lett. **86**, 886 (2001).
- [16] D. T. Fuchs *et al.*, Nature (London) **391**, 373 (1998).
- [17] S. Watauchi *et al.*, Phys. **C259**, 373 (1996).
- [18] A. E. Koshelev, Phys. Rev. Lett. **83**, 187 (1999).
- [19] S. E. Savel'ev, J. Mirković, and K. Kadowaki, Phys. Rev. B **64**, 94521 (2001).
- [20] M. Tachiki and S. Takahashi, Solid State Commun. **70**, 291 (1989).
- [21] In a wide angular range $90^\circ - 57.3^\circ/\gamma > \theta$, the equation $R(H_c, H_{ab}) = R(H_c, 0) + \nu(H_c, T)H_{ab}^2$ with $\nu(H_c, T) = (\partial^2 R(H_c, H_{ab})/\partial H_{ab}^2)|_{H_{ab}=0}$ can be used, since a linear term does not follow the symmetry restrictions. Thus, $H_c^R(H_{ab})$ should satisfy the equation $R(H_c^R(H_{ab}), 0) + \nu H_{ab}^2 = R(H_c^R(0), 0)$ with $R(H_c^R(0)) = R^*$ and $R^* = 10^{-3}\Omega$. The approximate solution of the equation, presented in the text, yields the phenomenological anisotropy $\gamma_{phen}(T, H_c^R(0)) = \sqrt{(\partial R(H_c, 0)/\partial H_c)|_{H_c=H_c^R(0)}/\nu H_c^R(0)}$.
- [22] J. Mirković *et al.*, Physica **C357**, 450 (2001).
- [23] L. L. Deamen *et al.*, Phys. Rev. B **47**, 11291 (1993).
- [24] We use the equation obtained in Ref. [23] for the Josephson coupling prevailing over the electromagnetic one which is valid if $\gamma s \lesssim \lambda_{ab}(T)$. The last condition is satisfied at $T > T^*$ with $T^*/T_c = 1 - \lambda_{ab}^2(T=0)/\gamma^2 s^2 = 0.8$ for $\lambda_{ab}(T=0) = 2000 \text{ \AA}$, $s = 15 \text{ \AA}$, $\gamma = 300$.